Iterative Learning Control for Laser Scanning based Micro 3D Printing

Han Woong Yoo [*,1] **Christoph Johannes Kerschner** [*,1]
Shingo Ito [*] **Georg Schitter** [*]

[*] *Automation and Control Institute (ACIN), TU Wien, Gusshausstr. 27-29, 1040 Vienna, Austria*
(e-mail: {yoo, kerschner, ito, schitter}@acin.tuwien.ac.at).

Abstract: This paper proposes an iterative learning control (ILC) for a micro stereo lithography (MSL) setup to enhance both the speed and the quality of 3D printing. The MSL setup is built based on a commercial confocal microscope while the scanners of both x and y axes are replaced with fast galvanometer scanners considering requirements of random trajectories in 3D printing application. With the stabilized galvanometer scanners, a frequency domain ILC is applied for a precise operation of desired 2D scanning trajectories. For fast scan trajectories up to 400 features per second of a 0.6 × 0.6 mm square, the RMS beam tracking error of the ILCs is reduced by a factor of 25.9 compared with a conventional feedback controllers, also significantly reducing the velocity variation. The printing results with the MSL setup also demonstrate that ILC can improve uniformity of line thickness as well as accuracy of the trajectory.

Keywords: Iterative learning control, 3D printing, Micro stereo lithography (MSL), Scanning MSL, Velocity fluctuation

1. INTRODUCTION

Additive manufacturing, also often called 3D printing, refers to a process by which materials are deposited layer by layer to build components (Horn and Harrysson (2012)). In recent years additive manufacturing received much attention due to increasing demands in the rapid prototyping and technology advancement, enabling design-driven manufacturing (Joshi et al. (2012)). The speed of 3D printing processes are critical not only for high throughput of the manufacturing process but also for design optimization by reducing cost and time of the design iteration (Vaezi et al. (2013); Tumbleston et al. (2015)).

Stereo Lithography (SL) technologies are one of the earliest additive manufacturing techniques, which uses light to cure the a liquid resin selectively by photopolymerization (Kodama (1981)). Compared to other additive manufacturing techniques, SL is most suitable for fabrication of micro-scale components, which is called micro stereolithography (MSL) due to high resolution, good surface quality, and no porosity (Vaezi et al. (2013)). By the light control mechanisms, MSL machines are categorized by projection MSL and scanning MSL (Vaezi et al. (2013)). Projection MSL typically uses a liquid crystal display (LCD) or a digital micromirror device (DMD) to create mask patterns for printing, providing extremely high printing speed for large and complex structures while the resolution of the outline is rough due to innate pixelated structure (Stampfl et al. (2016); Bertsch et al. (1997)). Scanning MSL machines uses moving the beam spot, which can generate fine finishing of the outlines, but it is slower than projection based MSL.

Scanning MSL machines often use galvanometer scanners due to their high flexibility and cost-effectiveness (Stampfl et al. (2016)). The quality of the printed lines also depends on the speed variation of the light spot, which is also considered as local exposure for the resin (Tumbleston et al. (2015)). For galvanometer scanners (Yoo et al. (2016)), however, the inertia of the rotor and the finite torque do not allow to have a constant speed at a sharp turnaround while the printing patterns typically contain such corners. One main approach is based on path planning that add a path for acceleration and deceleration to keep the target path in a constant velocity and turn off the laser during the added path (Stampfl et al. (2016); Yeung et al. (2016); Luo et al. (2017)). Another main approach is based on modulation of the laser power or pulsing frequency according to the beam velocity to compensate for the velocity variations (Yeung et al. (2016); Luo et al. (2017); Pothen et al. (2017)). Both techniques can improve line thickness variation, however the path planning approach needs much effort for users to generate a proper path (Pothen et al. (2017)) and requires a prior calibration of the laser beam for the defined scanning pattern, which can reduce the entire throughput of the MSL. So far, little attention has been paid to scanning controls to improve such beam velocity profiles in 3D printing.

This paper proposes an iterative learning control (ILC) for a micro stereo lithography (MSL) setup to enhance both the speed and accuracy of the repetitive scanning trajectories. ILC is a feedforward control that reduces tracking errors for desired trajectories by learning from the previous trials. Barton and Alleyne (2008) propose

[1] These authors contributed equally to this work.

Post-print version of the article: H. W. Yoo, C. J. Kerschner, S. Ito, G. Schitter, "Iterative Learning Control for Laser Scanning based Micro 3D Printing," *8th IFAC Symposium on Mechatronic Systems*, vol. 52, no. 15, pp 169-174, 2019. DOI: 10.1016/j.ifacol.2019.11.669

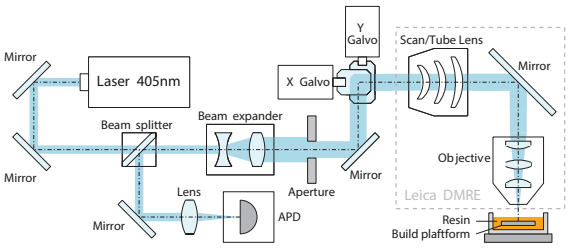

(a) Schematic diagram

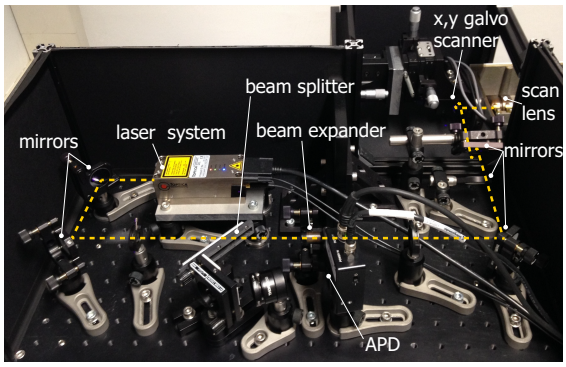

(b) Picture

Fig. 1. Schematic diagram and picture of the developed micro stereolithography setup.

ILCs for electrohydrodynamic jet (e-jet) based 3D printing to improve positioning accuracy of deposition system, and Hoelzle and Barton (2016) proposed spatial ILC considering 2D printed outcome. Yoo et al. (2016) propose ILC for galvanometer scanners in confocal laser scanning microscopy, showing improved tracking performance in a wide bandwidth. This paper extends the application of the ILC for galvanometer scanners to micro 3D printing, evaluating the benefits in the printing results. Due to simplicity in modeling, a frequency domain ILC (Li and Bechhoefer (2009); de Rozario et al. (2016)), also called inversion-based iterative control (IIC) (Kim and Zou (2013); D. Wang (2014); Ito et al. (2017a)), is used for the stabilized galvanometer scanners in the MSL setup. The ILC and the MSL setup is evaluated for a square shape test pattern to illustrate its benefits.

The paper is organized as follows. Section 2 describes the developed MSL setup based on a commercial microscope with a laser and two fast galvanometer scanners as key components. Feedback stabilization of the galvanometer scanners and the design of the frequency based ILC are described in Section 3. Section 4 presents experimental results with an analysis on pattern accuracy and beam velocity, and printing results of a single layer are discussed. Section 5 concludes the paper.

2. EXPERIMENTAL SETUP

Fig. 1 shows a schematic diagram and a picture of the MSL setup. The MSL setup is built based on a optical microscope (Leica DMRE, Leica Microsystems, Wetzlar, Germany) with an external laser, galvanometer scanners and associated optics. A diode laser system (iBeam Smart, 405 nm, 150 mW, digital bandwidth 250 MHz, Gräfeling, Toptica Photonics, Germany) emits laser light. The laser light passes a beam splitter (70:30, component from Leica SP2) and is expanded by a beam expander (3× beam expander, component from Leica SP2). Then the beam diameter is adjusted by a diaphragm (ID25, ThorLabs, Newton, NJ, USA) to fill the back focal plane of the microscope objective. After mirrors the laser beam coincides two galvanometer scanners, which are positioned at the back focal plane of the scan lens to move the focused beam in x- and y-direction. An objective (HC PL Fluotar, 10×, 0.3 NA, 1.5 mm × 1.5 mm field of view, Leica) focuses the beam onto the build platform in the resin container. Since the microscope is an upright type, the MSL setup is built in top-down architecture, where the laser cures the material from the top. The reflected light from the sample passes back through the microscope and is focused on an APD sensor (APD120, ThorLabs) by a lens (AC254-045-A1, $f = 45$ mm, ThorLabs) to detect the focal plane precisely.

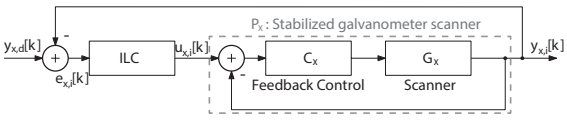

Fig. 2. Overall architecture of controllers for the x axis galvanometer scanner. The galvanometer scanner G_X is stabilized by a feedback controller C_X. At i-th iteration and time k, the ILC is applied as a feedforward controller to the an input signal $u_i[k]$ of the stabilized galvanometer scanner P_X, reducing the the error $e_i[k]$ of the encoder output $y_i[k]$ with respect to the desired output trajectory $y_d[k]$.

For 3D printing, in contrast to most optical scanning microscopes, the beam trajectories can be arbitrary due to the target structures to print, i.e the speed of the scanners in both x and y axis should be equally high. Two fast galvanometer scanners (6210H, Cambridge Technology, Lexington, MA, USA) are chosen, which are a moving magnet type with low rotor inertia and have the structural modes beyond 20 kHz (Yoo et al. (2016)). The galvanometer scanners are driven by custom-made current amplifiers with more than 50 kHz bandwidth, and sensor readout boards (678 rev.B, Cambridge Technology) to process the encoder output of the galvanometer scanner measuring the beam deflection angle.

3. CONTROL DESIGN

This section describes the control design for the x and y galvanometer scanners. Since the x or y galvanometer scanner are similar and have the same controller structure, the design is shown for one axis only. Fig. 2 describes an overall architecture of the controller for the x galvanometer scanner where G_X and C_X represent transfer functions of the open loop galvanometer scanner and a feedback controller, respectively. ILC is applied as a feedforward control to the stabilized galvanometer scanners P_X, which is called closed loop injection architecture (Butterworth

Post-print version of the article: H. W. Yoo, C. J. Kerschner, S. Ito, G. Schitter, "Iterative Learning Control for Laser Scanning based Micro 3D Printing," *8th IFAC Symposium on Mechatronic Systems*, vol. 52, no. 15, pp 169-174, 2019. DOI: 10.1016/j.ifacol.2019.11.669

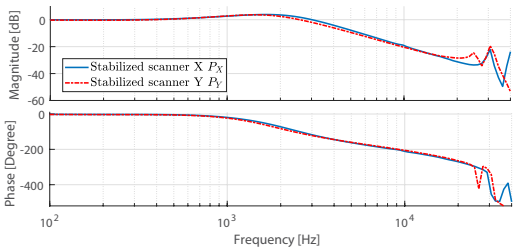

Fig. 3. Measured complimentary sensitivity function of the stabilized x- and y- galvanometer scanners.

et al. (2009)). Details of the feedback controller and the ILC are discussed in the following subsections.

3.1 Feedback Control for Stabilization

Because the galvanometer scanners is marginally stable, a feedback controllers is utilized for stabilization before applying ILC (Yoo et al. (2016)). Lead-lag controllers are used with a cross-over frequency of 2 kHz, i.e. $\omega_c = 2\pi \cdot 2000$, for enough gain and phase margin and low sensor noise for ILC. The transfer function of the designed feedback controller is

$$C_X(s) = \frac{1}{3|G_X(\omega_c)|} \frac{\omega_i}{\omega_{it}} \frac{(1 + {}^s/_{\omega_i})}{(1 + {}^s/_{\omega_{it}})} \frac{(1 + {}^s/_{\omega_d})}{(1 + {}^s/_{\omega_{dt}})}, \quad (1)$$

where the control parameters are set by $\omega_i = \omega_c/10$, $\omega_d = \omega_c/3$, $\omega_{dt} = 3\omega_c$, and $\omega_{it} = 2\pi \cdot 6$, based on PID tuning methods in (Munnig Schmidt et al. (2011)).

The designed feedback controllers are implemented in a real time control system (MicroLabBox, dSpace, Paderborn, Germany) with a FPGA board (DS1302, Kintex-7, dSpace) at a sampling frequency f_s of 1 MSps. The measured gain margins are 68.5 dB and 69.6 dB and the phase margins are 53° and 51° for the x and y galvanometer scanners, respectively. Fig. 3 shows complementary sensitivity function of the stabilized galvanometer scanners, measured by a dynamic signal analyzer (HP 3563A, Keysight technologies, Santa Rosa, CA, USA), showing the designed bandwidth of the feedback controllers at 2 kHz for both x and y galvanometer scanners. The resonances of the x scanners are at 31.26 kHz and 41.70 kHz and the resonances of y scanners are at 25.71 kHz and 31.55 kHz, respectively.

3.2 Iterative Learning Control

With the stabilizing feedback controller, an ILC is applied to compensate for gain and phase errors as well as periodic disturbances over a wide bandwidth (Yoo et al. (2016)). Assume that the desired output signal $y_{x,d}$ and the input by ILC $u_{x,i}$ at the i-th trial are periodic with a length N for an infinite time duration, i.e. the system is in a steady state (de Rozario et al. (2016); Yoo et al. (2016)). Then the encoder output $y_{x,i}$, the desired output $y_{x,d}$, and the control $u_{x,i}$ can be represented by a limited number of harmonic frequencies of the fundamental frequency $f_r = f_s/N$. The ILC can be designed in the frequency domain to compensates at this fundamental frequency and the harmonic frequencies only as (Li and Bechhoefer (2009); Kim and Zou (2013); de Rozario et al. (2016); Ito et al. (2017a))

$$U_{x,i+1}[n] = \begin{cases} U_{x,i}[n] + \rho \hat{P}_X^{-1}[n] E_{x,i}[n], & n \in S_{\tilde{N}} \\ 0 & n \notin S_{\tilde{N}}, \end{cases} \quad (2)$$

$$E_{x,i}[n] = Y_{x,i}[n] - Y_{x,d}[n], \quad (3)$$

where discrete Fourier transform (DFT) coefficients of the output and desired output signal are defined as

$$Y_{x,d}[n] = \sum_{k=0}^{N-1} y_{x,d}[k] e^{-j\frac{2\pi}{N}nk},$$
$$Y_{x,i}[n] = \sum_{k=0}^{N-1} y_{x,i}[k] e^{-j\frac{2\pi}{N}nk}, \quad (4)$$

where j denotes the imaginary number $j = \sqrt{-1}$, n is the index of harmonic frequencies for the fundamental frequency $\frac{2\pi}{N}$ in discrete time domain, and $S_{\tilde{N}}$ is a selected subset of the harmonic frequencies, i.e. $S_{\tilde{N}} \subset S_N = \{0, 1, \cdots, N-1\}$, which are the low order harmonic frequencies with good SNR (Elci et al. (1994); Ito et al. (2017a)). $\hat{P}_X$ is the modeled frequency response function of the stabilized galvanometer scanner P_X, and ρ denotes a learning gain to cope with modelling errors by sacrificing learning speed. Both finite numbers of harmonic frequencies and the learning gain are designed as a Q filter in ILC to meet the condition of monotonic convergence of ILC as (Norrlof and Gunnarsson (2002); de Rozario et al. (2016))

$$\left|1 - \rho P_X[n] \hat{P_X}^{-1}[n]\right| \leq 1, \quad \forall n \in S_{\tilde{N}}. \quad (5)$$

The input in the time domain at the next iteration, $u_{x,i+1}[k]$, is obtained by the inverse DFT with the finite harmonic frequencies as

$$u_{x,i+1}[k] = \frac{1}{N} \sum_{n}^{S_{\tilde{N}}} U_{x,i+1}[n] e^{-j2\pi kn/N}. \quad (6)$$

In contrary to the inversion of the transfer function, the frequency response function model is obtained by a direct inversion of the complex number at each harmonic frequency, which does not suffer from unstable inversion of non-minimum phase zeros (Ito et al. (2017b)). By assuming that the system P_X is linear time-invariant (D. Wang (2014)), the discrete frequency components of the inverse model can be obtained by a simple division in the frequency domain as

$$\hat{P}_X^{-1}[n] = \begin{cases} \dfrac{U_{x,1}[n]}{Y_{x,1}[n]}, & n \in S_{\tilde{N}}, \\ 0, & n \notin S_{\tilde{N}}, \end{cases} \quad (7)$$

where $Y_{x,1}[n]$ and $U_{x,1}[n]$ are frequency components of the measured trajectory $y_{x,1}[k]$ and the input signal $u_{x,1}[k]$ at the first iteration, respectively.

For the implementation of ILC with the synchronized laser controls, two DAQ systems (U2531A, $f_s = 1$ Msps, AI 14 bit, AO 12 bit, Keysight Technologies) are used to generate simultaneous periodic signal. The first DAQ card receives the encoder signals from both axes and provides the input by ILC to the real time controller. The second DAQ generates a laser enable signal, which digitally turns on and off the laser according to the scanning trajectories.

Post-print version of the article: H. W. Yoo, C. J. Kerschner, S. Ito, G. Schitter, "Iterative Learning Control for Laser Scanning based Micro 3D Printing," *8th IFAC Symposium on Mechatronic Systems*, vol. 52, no. 15, pp 169-174, 2019. DOI: 10.1016/j.ifacol.2019.11.669

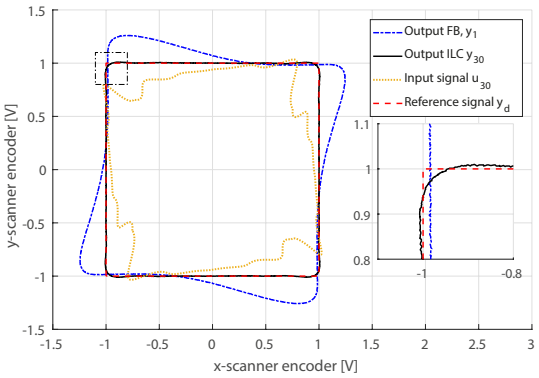

(a) 2D XY plot

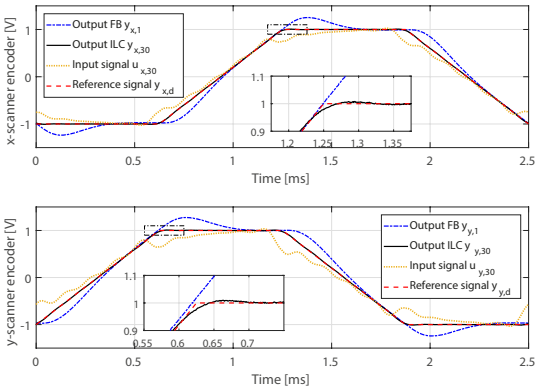

(b) X and Y trajectory

Fig. 4. Measured trajectories of the feedback controllers and the ILC for the desired output at 400 features/s on (a) xy plane and (b) along the time axis. The input of the ILC is also drawn as well.

4. VALIDATION OF ILC

This section presents experimental results of the frequency domain ILC for the x and y galvanometer scanners in comparison to the designed feedback controllers. A square trajectory is chosen for the desired output $y_{x,d}$ as a representative fine outline pattern in 3D printing at a rate of 100, 200 and 400 features/s. The ILC runs up to 30 iterations for experimental verification of the monotonic convergence of the error. Initial input by ILC is set by the desired output, i.e. $u_{x,1} = y_{x,d}$. This means that the encoder output $y_{x,1}$ at the first iteration corresponds to that of the feedback controller only while $y_{x,30}$ shows the output improved by the ILC. Considering the convergence of ILC with model errors in Eq. (5), the compensated harmonic frequencies for the ILC are limited up to 8 kHz, i.e. 80, 40 and 20 harmonic frequencies for 100, 200 and 400 features/s scanning trajectories, respectively. The learning gain ρ is set to 0.4.

4.1 Tracking Performance

Fig. 4a shows the encoder outputs on the xy plane for the desired output signal y_d at 400 features/s. The encoder output by the ILCs (black solid line) shows a square trajectory with small rounded corners while about 12.5 % overshoot is observed for each axis with the feedback controller (blue dash-dotted line). The generated input by the ILCs at the 30th iteration (orange dotted lines) shows a significant change of the input to the stabilized galvanometer scanners. Fig. 4b describes the trajectories along the time axis, showing an overshoot after the transition of the scanning motion by the feedback controllers. The ILC input u_{30} shows a non-causal behavior by design, compensating for the upcoming overshoot before the turnaround occurs. Fig. 5 shows the power spectral density of the error trajectories at 400 features/s with measured encoder noise floor (red dotted line with asterisks). The error frequency components of the ILC (black solid line with circles) are significantly reduced up to the 19th harmonic frequency while the error frequency components of the feedback controller (blue dashed line with diamonds) remain high for all harmonic frequencies.

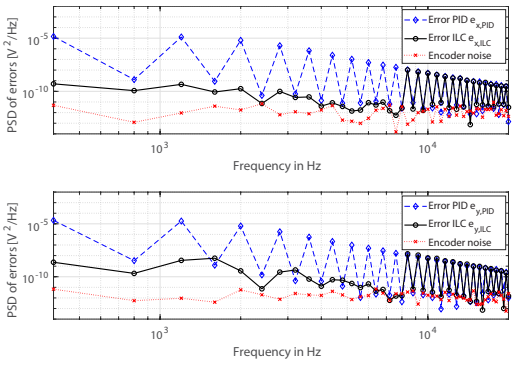

Fig. 5. Measured power spectral density of error trajectories of both x and y axis with the feedback controller and the ILC with measured encoder noise.

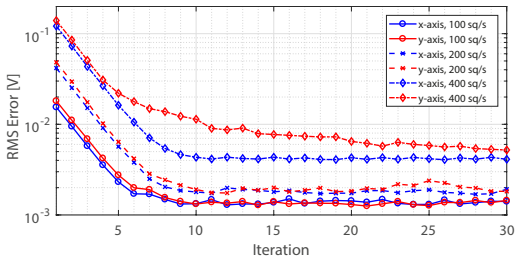

Fig. 6. Learning transient of the ILC for the rate of the 100, 200, and 400 features/s. The red and blue lines displays the RMS error of the x- and y- actuators, respectively.

Table 1. RMS and peak to peak errors. [mV]

RMS (PP)		100 feat./s	200 feat./s	400 feat./s
x axis	FB	15.49 (126.82)	41.86 (243.10)	121.18 (491.46)
	ILC	1.41 (12.91)	1.92 (21.24)	4.11 (41.99)
y axis	FB	17.98 (142.40)	48.29 (275.90)	139.59 (532.96)
	ILC	1.45 (12.98)	1.8207 (20.02)	5.21 (44.43)

Post-print version of the article: H. W. Yoo, C. J. Kerschner, S. Ito, G. Schitter, "Iterative Learning Control for Laser Scanning based Micro 3D Printing," *8th IFAC Symposium on Mechatronic Systems*, vol. 52, no. 15, pp 169-174, 2019. DOI: 10.1016/j.ifacol.2019.11.669

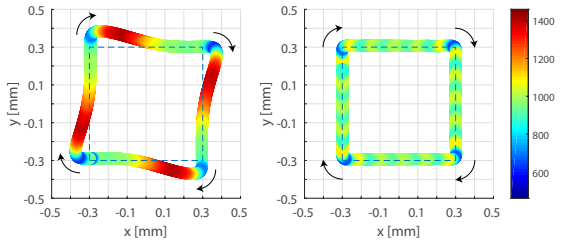

Fig. 7. Beam velocity plot of the trajectory at 400 features/s (left) only with feedback control and (right) with ILC. The beam velocity is depicted as color with the unit of mm/s. Black arrows indicate the direction of beam scanning.

Table 2. Mean, standard deviation, minimum and maximum of velocity profiles. [mm/s]

		100 feat./s	200 feat./s	400 feat./s
Mean(STD)	FB	245(27)	502(75)	1061(202)
	ILC	239(12)	477(26)	947(91)
(Max.,Min.)	FB	(158,351)	(311,697)	(623,1401)
	ILC	(156,280)	(344,535)	(640,1101)

Fig. 6 shows the learning transient in RMS errors of the measured encoder output for the scan rate of 100, 200, and 400 features/s. In most cases except the y galvanometer scanner at 400 features/s, the RMS errors converge to a minimum within 10 iterations and stay at the same level for the rest of the measurement. For the y galvanometer scanner at 400 features/s, the error converges slower due to large noise during the model identification while the error converges to a minimum around the 30th iteration as well. The final RMS errors vary by the scan rates because the number of compensated harmonics are less as the scan rate is higher. The resulting RMS and peak to peak beam tracking errors of the ILCs and the feedback controllers are listed in Table 1, showing a significant reduction by ILC by a factor up to 25.9 compared with the feedback controller.

4.2 Beam Velocity Evaluation

Especially for MSL, beam velocity is analyzed for the uniformity evaluation of printed lines (Tumbleston et al. (2015)). From the square trajectories with 0.6×0.6 mm, the target velocities are 240, 480, and 960 mm/s for 100, 200, and 400 features/s. In practice it is difficult to attain a constant speed due to turnarounds at each corner. To obtain the beam velocity, the encoder outputs are differentiated and then filtered by a 4th order low pass Butterworth filter with a bandwidth of 20 kHz in a zero phase manner to remove high frequency errors by differentiation and to keep enough frequency contents of the trajectory errors. Then the beam velocity is calculated from the velocities of each x and y axis. The encoder outputs are scaled by 0.3 mm/V to compare to the printing results in the next subsection.

Fig. 7 shows two color-coded beam velocity plots based on the measured encoder outputs with the feedback controllers (left) and the ILC (right) at 400 features/s. The beam velocity by the feedback controllers reaches up to

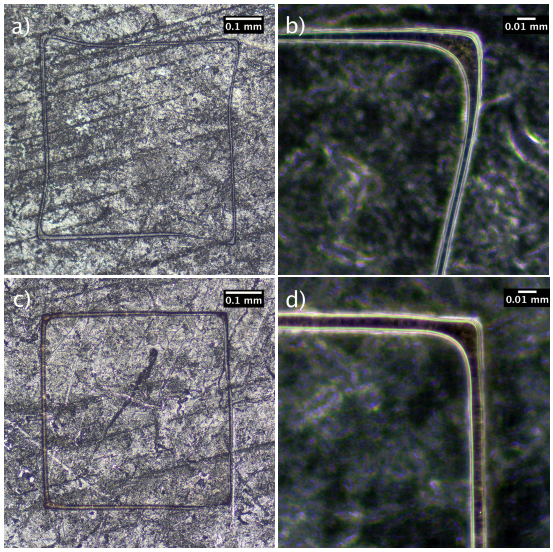

Fig. 8. Printing results of the square pattern at 200 feat./s on a steel disk. Bright field images (a,c) and zoomed dark field images (b,d) of the printed patterns with feedback control (a,b) and with ILC (c,d).

1401 mm/s after turnaround over an half of each edge. In contrast, ILC shows smaller velocity peak up to 1101 mm/s for all edges with residual high frequencies. Table 2 provides detail information about the velocity profiles according to the scan rates. ILC provides up to 34.6 % less standard deviation of the beam velocity and suppress the maximum velocity error with respect to the target velocity from 45.8 % to 14.6 % at 400 features/s. In case of the feedback controllers, the mean velocities are increased from the target velocity since the trajectories become longer by overshoot. In case of the ILCs, small reductions of the mean velocities from the target velocity are also observed since the trajectories shrink due to the realization of the sharp corners.

4.3 Printing Results

This section describes the printing results with the feedback controllers and the ILCs by the developed MSL setup. The same square trajectory is used with a size of 0.6 mm × 0.6 mm, corresponding to the amplitude of the 1 V and 1.44 V for x- and y- encoder signals. Since only a 2D printing is considered, only a thin layer of resin (Envisiontec R11) between a steel plate and a transparent polytetrafluoroethylene (PTFE) film is prepared for polymerization. The laser power is set to 30 mW and the laser is turned on during a single scan of the square trajectory. After printing and draining the rest of the resin, the sample is carefully cleaned with pure ethanol. The printed patterns are imaged by an optical microscope (Axio Scope.A1, Carl Zeiss, Oberkochen, Germany).

Fig. 8 illustrates the printing results of single line printing with the feedback controllers (a,b) and with the ILC (c,d) at 200 features/s. As shown in Fig. 4a, a distortion of the square pattern by the feedback controllers and its

Post-print version of the article: H. W. Yoo, C. J. Kerschner, S. Ito, G. Schitter, "Iterative Learning Control for Laser Scanning based Micro 3D Printing," *8th IFAC Symposium on Mechatronic Systems*, vol. 52, no. 15, pp 169-174, 2019. DOI: 10.1016/j.ifacol.2019.11.669

compensation by ILC are observed in Fig. 8a and 8c. Figure 8b and 8d show zoomed dark field images around a corner of the square pattern, showing the thickness of the printed line distinctly. The line thickness in the feedback controller case varies before and after the corner as a result of inhomogeneous curing due to beam velocity variations. In contrast, ILC shows relatively uniform thickness along the corner by small fluctuation of the beam velocity. This illustrates that ILC is beneficial in the high speed 3D printing of MSL not only for accurate and precise patterning for period trajectories but also for more uniform line thickness by decreasing beam velocity variations.

5. CONCLUSION

This paper investigates an integration of iterative learning control on a laser scanning based MSL to improve precision of the printed pattern as well as line thickness uniformity. A MSL setup is built based on a commercial confocal microscope by adding two high speed galvanometer scanners and a 405 nm diode laser. The galvanometer scanners are first stabilized by feedback controllers, and a frequency domain ILC is applied to compensate for the errors at the harmonic frequencies up to 8 kHz. As a test trajectory, a 2D square pattern is chosen and applied in a periodic manner at rates of 100, 200 and 400 features/s to verify benefits of the ILC as compared to the designed feedback control. Experimental results show that ILC reduces the RMS beam tracking errors by a factor of up to 25.9 compared with the feedback controllers. Additionally, the maximum velocity errors are reduced from 45.8 % to 14.6 % with respect to the target velocity. The printing results show the benefits of the ILC by the accurate patterning as well as more uniform line thickness.

ACKNOWLEDGEMENTS

The authors thank Prof. Jürgen Stampfl and Bernhard Busetti for their suggestions and supports for materials and printing procedure.

REFERENCES

Barton, K.L. and Alleyne, A.G. (2008). A Cross-Coupled Iterative Learning Control Design for Precision Motion Control. *IEEE Trans. on Cont. Syst. Tech.*, 16(6), 1218–1231.

Bertsch, A., Zissi, S., J., S.C., and André (1997). Microstereophotolithography using a liquid crystal display as dynamic mask-generator. *Microsyst. Technol.*, 3(2), 42–47.

Butterworth, J.A., Pao, L.Y., and Abramovitch, D.Y. (2009). A comparison of control architectures for atomic force microscopes. *Asian J. of Control*, 11(2), 175–181.

D. Wang, Y. Ye, B.Z. (2014). *Practical Iterative Learning Control with Frequency Domain Design and Sampled Data Implementation*. Springer.

de Rozario, R., Fleming, A.J., and Oomen, T. (2016). Iterative control for periodic tasks with robustness considerations, applied to a nanopositioning stage. *IFAC-PapersOnLine*, 49(21), 623 – 628.

Elci, H., Longman, R.W., Phan, M., Juang, J.N., and Ugoletti, R. (1994). Discrete frequency based learning control for precision motion control. *Proc. of IEEE Int. Conf. on Syst., Man and Cybern.*, 3, 2767–2773 vol. 3.

Hoelzle, D.J. and Barton, K.L. (2016). On Spatial Iterative Learning Control via 2-D Convolution: Stability Analysis and Computational Efficiency. *IEEE Trans. on Cont. Syst. Tech.*, 24(4), 1504–1512.

Horn, T. and Harrysson, O. (2012). Overview of current additive manufacturing technologies and selected applications. *Sci. Prog.*, 95(3), 255–282.

Ito, S., Yoo, H.W., and Schitter, G. (2017a). Comparison of modeling-free learning control algorithms for galvanometer scanners periodic motion. *IEEE Int. Conf. on Adv. Intell. Mechatron. (AIM)*.

Ito, S., Neyer, D., Steininger, J., and Schitter, G. (2017b). Dual Actuation of Fast Scanning Axis for High-speed Atomic Force Microscopy. *IFAC-PapersOnLine*, 50(1), 7633–7638.

Joshi, P., Dehoff, R., Ott, R., Love, L., and Blue, C. (2012). Direct digital additive manufacturing technologies: Path towards hybrid integration. *Future of Instrum. Int. Workshop (FIIW)*, 1–4.

Kim, K.S. and Zou, Q. (2013). A modeling-free inversion-based iterative feedforward control for precision output tracking of linear time-invariant systems. *IEEE/ASME Trans. on Mechatron.*, 18(6), 1767–1777.

Kodama, H. (1981). Automatic method for fabricating a three-dimensional plastic model with photo- hardening polymer. *Rev. Sci. Instrum.*, 52(11), 1770–1773.

Li, Y. and Bechhoefer, J. (2009). Model-free iterative control of repetitive dynamics for high-speed scanning in atomic force microscopy. *Rev. Sci. Instrum.*, 80(1), 013702.

Luo, X., Li, J., and Lucas, M. (2017). Galvanometer scanning technology for laser additive manufacturing. In *SPIE Laser 3D Manuf. IV*, 1009512.

Munnig Schmidt, R., Schitter, G., and van Eijk, J. (2011). *The Design of High Performance Mechatronics*. Delft University Press.

Norrlof, M. and Gunnarsson, S. (2002). Time and frequency domain convergence properties in iterative learning control. *Int. J. Control*, 75(14), 1114–1126.

Pothen, M., Winands, K., and Klocke, F. (2017). Compensation of scanner based inertia for laser structuring processes. *J. of Laser Appl.*, 29(1), 012017.

Stampfl, J., Liska, R., and Ovsianikov, A. (2016). *Multiphoton Lithography: Techniques, Materials, and Applications*. John Wiley and Sons, New York.

Tumbleston, J.R., Shirvanyants, D., Ermoshkin, N., Janusziewicz, R., Johnson, A.R., Kelly, D., Chen, K., Pinschmidt, R., Rolland, J.P., Ermoshkin, A., Samulski, E.T., and DeSimone, J.M. (2015). Continuous liquid interface production of 3D objects. *Science*, 347(6228), 1349–1352.

Vaezi, M., Seitz, H., and Yang, S. (2013). A review on 3D micro-additive manufacturing technologies. *Int. J. of Adv. Manuf. Technol.*, 67(5), 1721–1754.

Yeung, H., Neira, J., Lane, B., Fox, J., and Lopez, F. (2016). Laser path planning and power control strategies for power bed fusion systems. In *Proc. 27th Annu. Int. Solid Freeform Fab. Symp.*, 113–127.

Yoo, H.W., Ito, S., and Schitter, G. (2016). High speed laser scanning microscopy by iterative learning control of a galvanometer scanner. *Control Eng. Pract.*, 50, 12 – 21.

Post-print version of the article: H. W. Yoo, C. J. Kerschner, S. Ito, G. Schitter, "Iterative Learning Control for Laser Scanning based Micro 3D Printing," *8th IFAC Symposium on Mechatronic Systems*, vol. 52, no. 15, pp 169-174, 2019. DOI: 10.1016/j.ifacol.2019.11.669